Expanded View Figures

Figure EV1. Purification and characterization of active His-tagged SaHPF protein.

A Elution profile of SaHPF after Ni sepharose affinity chromatography. Fractions containing mostly absorbance at 280 nm were pooled (pool 1) separately from those containing mostly absorbance at 260 nm (pool 2). Each pool was subjected to size-exclusion chromatography.

B Elution profile of pool 1 after size-exclusion chromatography. Two peaks contained SaHPF: "peak 1" corresponds to pure protein (size ~50 kDa, suggesting the presence of SaHPF as a dimer); "peak 2" contains an extra absorbance at 260 nm and eluted at a position near 1 column volume, possibly due to interaction of this pool with the resin.

C Native PAGE of samples shown in (B), indicating that both peaks contain SaHPF dimers (~55 kDa).

D, E Sucrose-density gradient centrifugation profiles demonstrate the higher efficiency of "peak 2" in ribosome dimerization.

F Same as (B) for pool 2 after size-exclusion chromatography. Here, peak 1 is smaller and peak 2 contains an extra absorbance at 260 nm. Peak 2 was collected and used for dimerization of ribosomes.

G Sucrose-density gradient centrifugation profile obtained with peak 2 highlighted in (F).

H Calibration graph of Superdex 75 10/300 GL column according to the manufacturer.

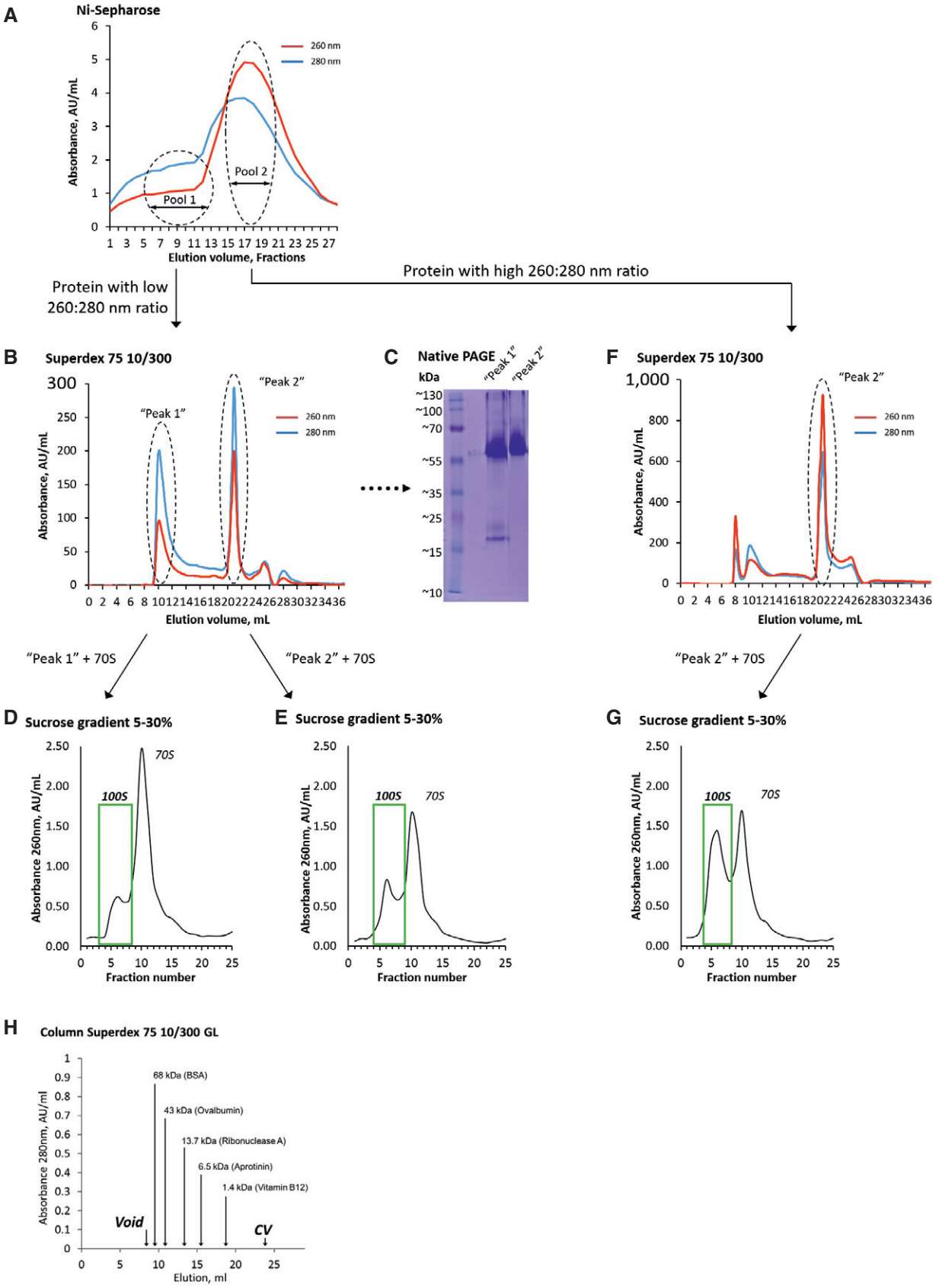

Figure EV1.

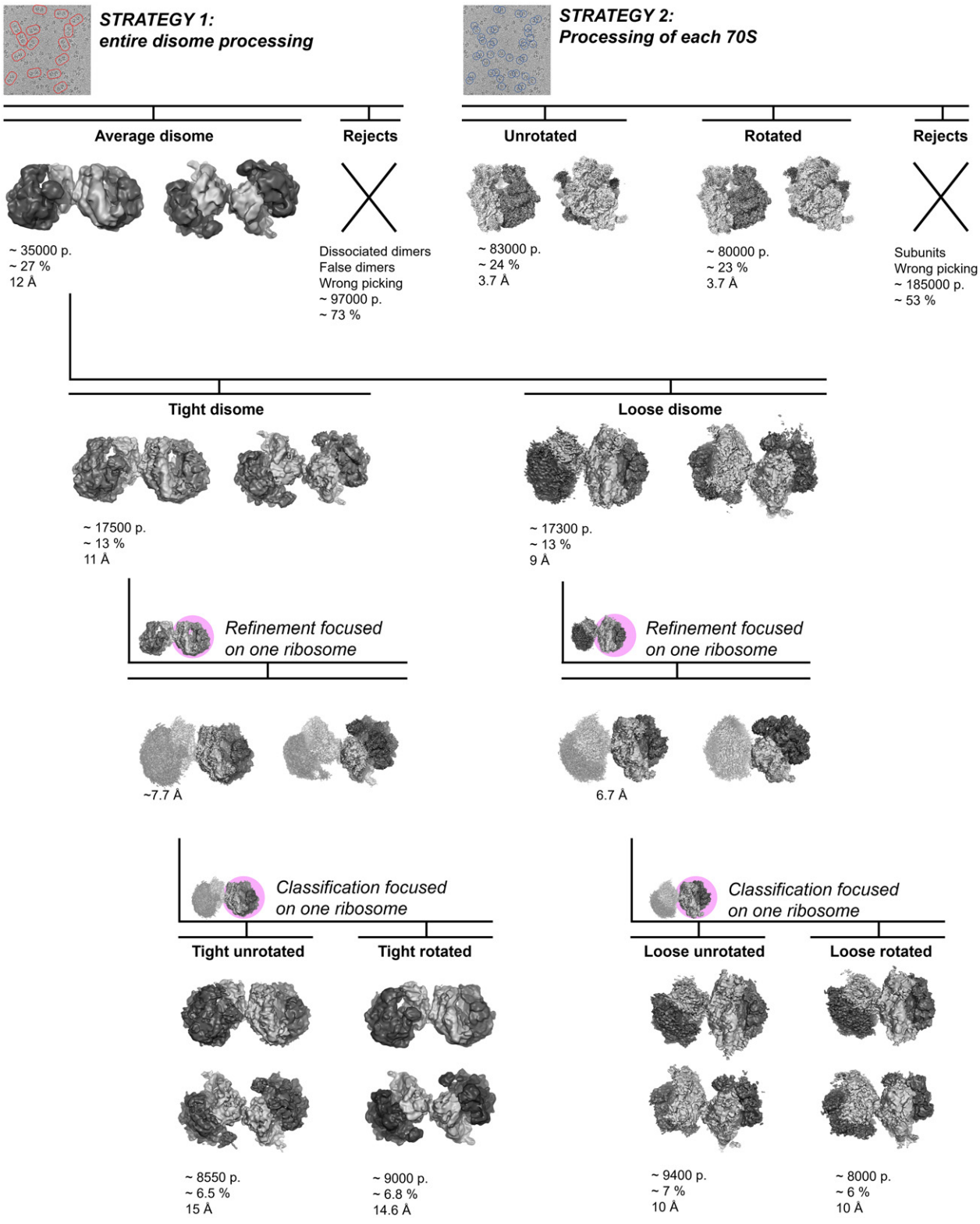

Figure EV2. Sorting out various classes of ribosomes within a dimer.
Strategy 1: Cryo-EM 3D particle sorting reveals two types of disome reconstructions after several runs of classification. Strategy 2: 3D reconstruction of each 70S revealed heterogeneity of the disomes. The total number of particles (p) used for the 3D reconstructions is indicated below each structure, along with the percentage calculated over the total number of particles, and the final average resolution of each class after refinement.

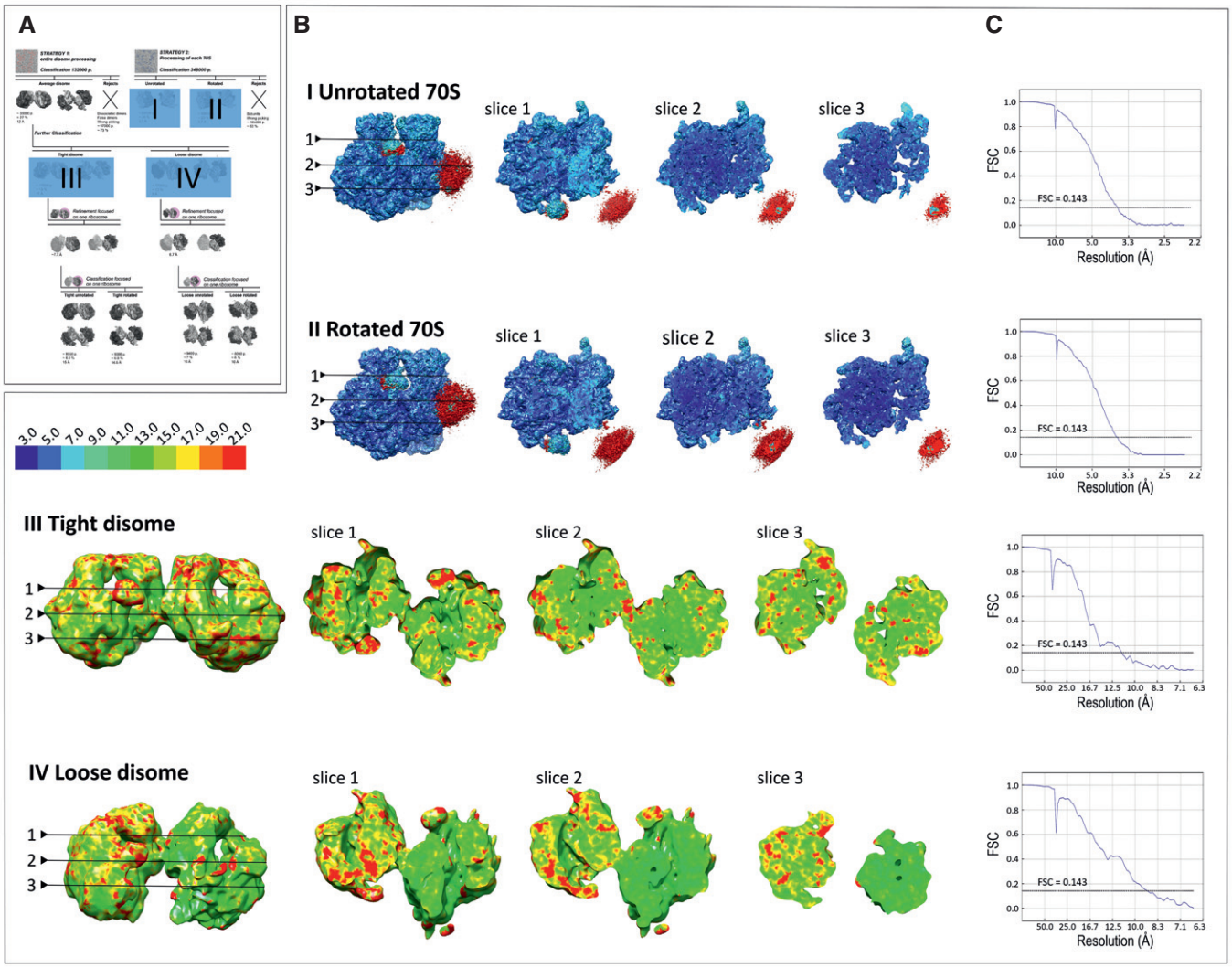

Figure EV3. Local resolution estimation of cryo-EM density maps.

A Miniaturized scheme of cryo-EM 3D particle sorting (shown in Fig EV2) highlighting 3D reconstructions (I–IV) used for local resolution estimation.

B Local resolution (rainbow scale) displayed on representative slices of the density maps I–IV.

C Fourier shell correlation (FSC) curve indicating the overall resolution of the cryo-EM maps I–IV.

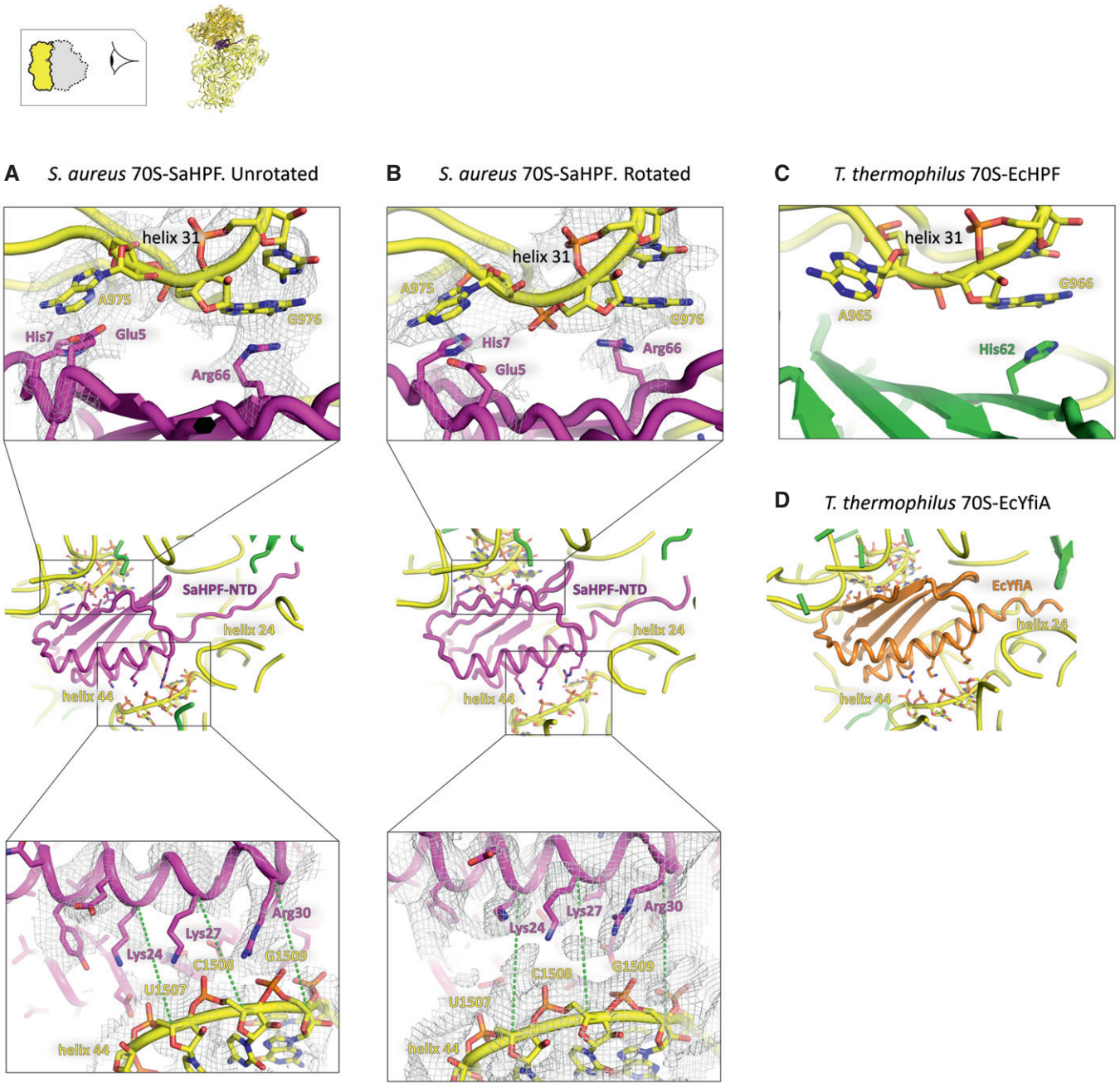

Figure EV4. Comparison of SaHPF-NTD-ribosome contacts between unrotated and rotated ribosomes, as well as with EcYfiA and EcHPF.

A Binding site of SaHPFNTD in the unrotated state. Amino acids of the NTD and nucleotides within 5 Å of one another in the head and body of the 16S rRNA are shown as sticks. The insets show a close-up of the interface between the β sheet and helix 31 (top; unfiltered map), and between positively charged amino acids in the α helical domain and helix 44 (bottom; unfiltered map). Green dashed lines are drawn from the same protein and backbone atoms in the two structures, in order to help visualize conformational dynamics that occur upon rotation.

B Same as panel (A), but for the rotated state. Green dashed lines are drawn from the same protein and backbone atoms in the two structures, in order to help visualize conformational dynamics that occur upon rotation.

C Same as the top view in panels (A and B), but for EcHPF in the *T. thermophilus* ribosome (PDB ID 4V8H; Polikanov *et al*, 2012).

D Same as the middle view in panels (A and B), but for EcYfiA in the *T. thermophilus* ribosome (PDB ID 4V8I; Polikanov *et al*, 2012).

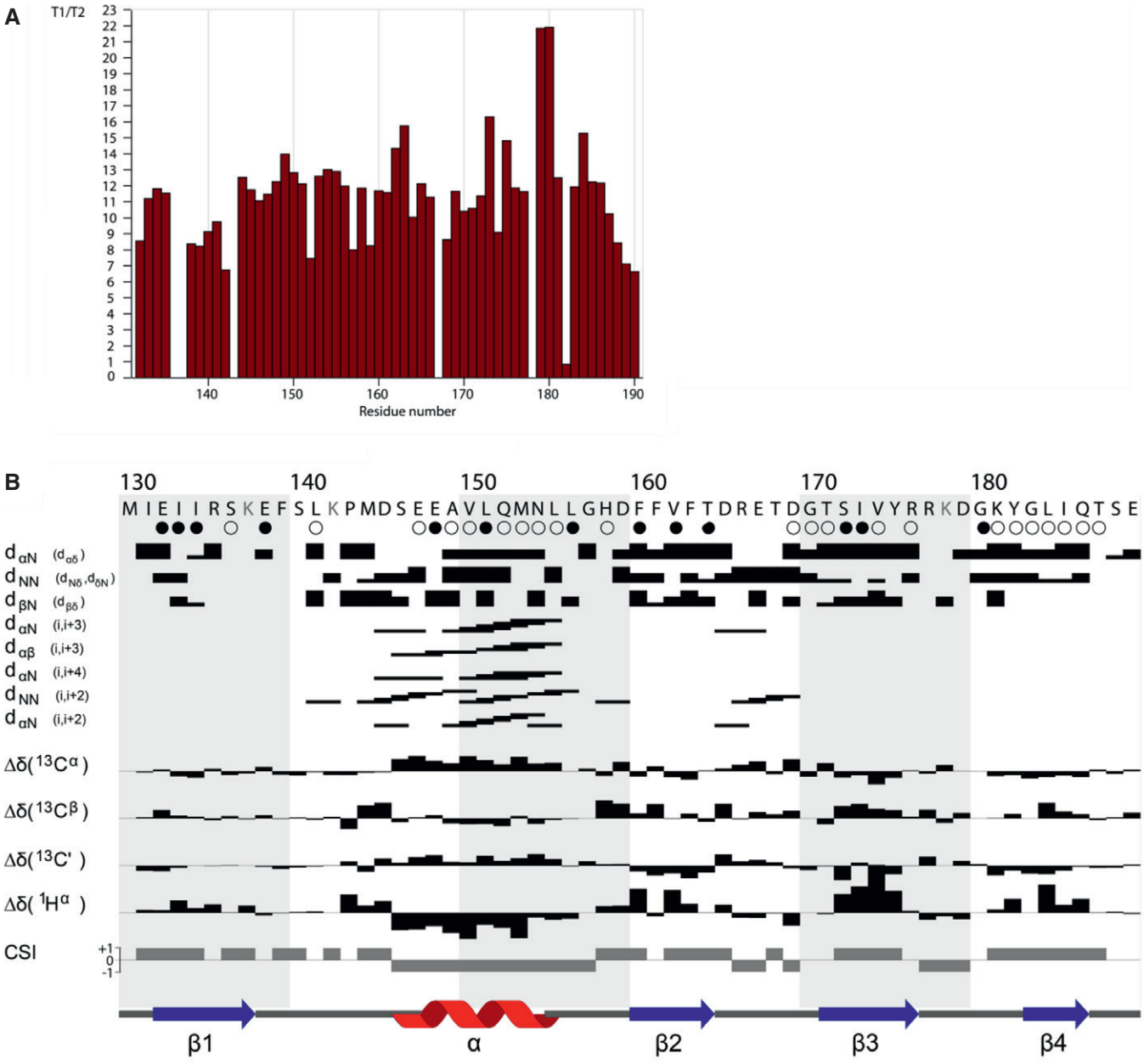

Figure EV5. SaHPF-CTD forms a dimer in solution.

A T1/T2 relaxation time ratio for SaHPF-CD residues (130–190).

B Summary of the sequential and medium-range NOEs, chemical shift index (CSI; Berjanskii & Wishart, 2005), and TALOS secondary structure. Residues shown in gray have not been detected in ^{15}N–^{1}H heteronuclear NMR spectra. The cartoons represent the portions of the SaHPF-CD predicted by TALOS to be α-helical (red) or β-strand (blue). Slowly and intermediate exchanging protons are identified by filled and empty circles, respectively.